Mode switching in organisms for solving explore-vs-exploit problems

Debojyoti Biswas^{1,*}, Andrew Lamperski², Yu Yang³, Kathleen Hoffman⁴, John Guckenheimer⁵, Eric S. Fortune⁶, and Noah J. Cowan^{1,3,*}

³Department of Mechanical Engineering, Johns Hopkins University, Baltimore, MD, USA. ⁴Department of Mathematics and Statistics, University of Maryland, Baltimore County, Baltimore, MD, USA.

⁵Department of Mathematics, Cornell University, Ithaca, NY, USA.
⁶Federated Department of Biological Sciences, New Jersey Institute of Technology, Newark, NJ, USA.

*e-mail: dbiswas2@jhu.edu **e-mail: ncowan@jhu.edu

Abstract

Tradeoffs between producing costly movements for gathering information ("explore") and using previously acquired information to achieve a goal ("exploit") arise in a wide variety of problems, including foraging, reinforcement learning, and sensorimotor control. Determining the optimal balance between exploration and exploitation is computationally intractable, necessitating heuristic solutions. Here we show that the electric fish Eigenmannia virescens uses a salience-dependent mode-switching strategy to solve the explore–exploit conflict during a refuge tracking task in which the same category of movement (fore-aft swimming) is used for both gathering information and achieving task goals. The fish produced distinctive non-Gaussian distributions of movement velocities characterized by sharp peaks for slower, task-oriented "exploit" movements and broad shoulders for faster, "explore" movements. The measures of non-normality increased with increased sensory salience, corresponding to a decrease in the prevalence of fast explore movements. We found the same sensory salience-dependent mode-switching behavior across ten phylogenetically diverse organisms, from amoebae to humans, performing tasks such as postural balance and target tracking. We propose a state-uncertainty-based mode-switching heuristic that (1) reproduces the distinctive velocity distribution, (2) rationalizes modulation by sensory salience, and (3) outperforms the classic persistent excitation approach while using less energy. This mode-switching heuristic provides insights into purposeful exploratory behaviors in organisms, as well as a framework for more efficient state estimation and control of robots.

Main

Organisms display complex patterns of movement that arise from the interplay between obtaining information ("explore")^{1–3} and using current information ("exploit").⁴ Exploratory movements to gain information, and exploitative movements to achieve the task at hand, are often mediated by the same motor systems. For example, the weakly electric glass knifefish (*Eigenmannia virescens*) produces both information-seeking exploratory movements^{2,3,5} and goal-driven exploitative movements to remain within a refuge^{6,7} using the same ribbon-fin locomotor system.^{8,9} Both of these types of movement occur in a single linear dimension, along the rostrocaudal axis. This behavior makes E. virescens an excellent model system with which to investigate the interplay between explore and exploit movements:

¹Laboratory for Computational Sensing and Robotics, Johns Hopkins University, Baltimore, MD, USA.

²Department of Electrical and Computer Engineering, University of Minnesota, Minneapolis, MN, USA.

within a fixed refuge, fish produce ancillary back and forth exploratory movements to sense the refuge, 2, 3, 5 but these back and forth (explore) movements conflict with the corrective movements (exploit) required for station keeping.

Resolving this conflict between explore movements⁵ versus goal-directed exploit movements is a computationally intractable optimization problem.^{10–12} How do organisms resolve the explore–exploit conflict? A simple heuristic to solve this problem would be for an organism to perform goal-directed exploit movements while superimposing continuous small exploratory sensing movements—in other words to use a persistent excitation approach.¹³ Indeed, this heuristic has proven effective (if suboptimal) as an engineering approach to solve the explore–exploit problem of identifying states and parameters of a dynamical system during task execution.¹³ If organisms were to employ such a strategy, they would produce movement statistics that correspond to a single behavioral mode (e.g., a single component Gaussian distribution) that continuously superimposes explore and exploit behavior.

In contrast, we discovered that *E. virescens* does not use a persistent excitation strategy; instead, it exhibits a mode-switching strategy between fast, active-sensing movements (explore) and slow, corrective movements (exploit). This mode switching is modulated by sensory salience (Fig. 1–2). To assess the generality of this mode-switching strategy we investigated ten additional tasks performed by ten species ranging from amoebae to humans, ^{14–22} using five major sensing modalities—vision, audition, olfaction, tactile sensing and electrosensation (Fig. 4). Based on this extensive reanalysis we found that such mode switching—and its dependence on sensory salience—is found across diverse behaviors, taxa, and sensing modalities (Fig. 4). Inspired by this widespread biological strategy, we propose an engineering heuristic for selecting behavioral modes based on state uncertainty (Fig. 5), and show that this heuristic captures key features of mode switching found across organismal models. Furthermore, we show that this mode-switching heuristic can achieve better task-level performance, and do so with less control effort, than the conventional persistent excitation strategy.

E. virescens exhibited fast and slow behavioral modes

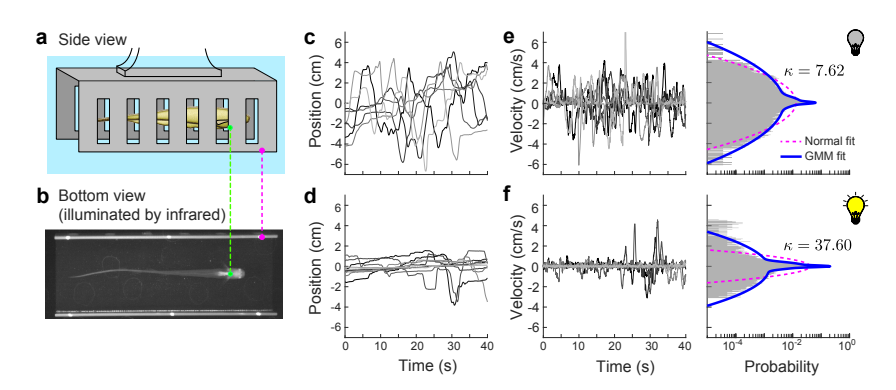


Fig. 1. Velocity distributions are broad-shouldered. (a) Side view (schematic) and (b) bottom view (infrared image) of a fish inside a stationary refuge. The bright ventral patch on the fish was tracked (green dot) as the fish swam inside the refuge (magenta dot). (c,d) Position traces during (c) lights-off trials (n=7), and (d) lights-on trials (n=10) from a single representative fish. (e,f) Corresponding velocity traces during lights-off trials (left) and velocity histogram (right) over the same range of velocities for (e) lights-off, and (f) lights-on trials, with the kurtosis value κ indicated; note that the time and probability scales of the horizontal axes are shown below panel (f). A three-component Gaussian mixture model (GMM; blue solid curve) fit the data better than the normal fit (magenta dashed curve) as indicated by the lower Kullback-Leibler divergence and Bayesian information criterion values; see Extended Data Table 1 for statistical details. One lights-off trial with large positive velocity is truncated; see Extended Data Fig. 1a,b for full version.

We examined the behavior of individual E. virescens as they performed untrained station keeping within a fixed refuge (Fig. 1a,b). Station keeping requires only small corrective movements; therefore any significant movements by the fish are attributed to information-seeking, exploratory movement.^{2,3,5} Previous work²³ has demonstrated that E. virescens use both vision and electrosense for station-keeping. Hence varying light level is an experimental mechanism to examine the effect of visual salience on the selection between explore and exploit movements.

We measured the movements of five individual fish in $40 \,\mathrm{s}$ duration station-keeping trials, in two lighting conditions: lights "off" trials had low illumination ($\sim 0.3 \,\mathrm{lx}$, Supplementary Video 1), and lights "on" trials had bright

illumination (~80 lx, Supplementary Video 2). We conducted between 7 and 10 trials per condition per fish. We discarded trials in which the fish changed its swimming direction or exited the refuge. Consistent with prior studies, ^{2,5} fish moved significantly more in lights-off conditions than in lights-on conditions (Fig. 1c,d, Extended Data Fig. 1a–d). However, these previous analyses ^{2,5} focused on tracking performance using analytical methods including Fourier analysis and root-mean-square metrics that masked the temporal structure of active sensing movements that we seek to undestand in this paper.

We found the patterns of fish swimming velocities were consistent with a mode-switching strategy. The distribution of velocities (v) featured a sharp peak around v = 0 with "broad" shoulders for faster movements (Fig. 1e,f, right). These empirical distributions differed from a Gaussian distribution in two ways: (i) the distinct central peak, and (ii) the broad shoulders corresponding to the faster movements. The central peak (near zero velocity) represents slow movement, and the broad shoulders represent faster movement. These behavioral modes are associated with exploit and explore respectively, as discussed in greater detail below.

The two behavioral modes were significantly better approximated by three-component Gaussian mixture models (GMMs) than by single component models (Fig. 1e,f, right). This was shown by three measures, namely Kullback-Leibler (K-L) divergence, Bayesian information criterion (BIC), and closeness of quantile-quantile (Q-Q) plots to the reference line (Extended Data Table 1, Extended Data Fig. 1e,f, Supplementary Fig. 1). The three component GMMs generally comprised a sharp central Gaussian peak, capturing slow, task-oriented station-keeping movements, and two Gaussian "shoulders", capturing faster, positive (forward) and negative (backward) exploratory movements. We found that only modest improvements in the fit of the GMMs occurred when using more than three components (Extended Data Fig. 1g).

The fast mode movements increased in frequency in lights-off trials, increasing the relative prominence of the "shoulders". For example, Fig. 1e,f show representative data from one fish in which there were 48 fast movements with lights off (Fig. 1e, left) but only 13 fast movements with lights on (Fig. 1f, left). Interestingly, the overall higher proportion of fast velocities in lights-off trials leads to a surprising result, namely higher kurtosis values for lights-on versus lights-off trials (Extended Data Fig. 1h). In other words, the increase in frequency of fast motions in the dark leads to a decrease in the relative prominence of the central, task-oriented velocity peak at v = 0, so that the overall distribution is closer to Gaussian, and the kurtosis trends toward 3.

We found that the trend towards a Gaussian distribution of movement velocities in lights-off trials (reduced sensory salience) to be surprising because the exploratory movements for actively sensing the environment are associated with a nonlinear requirement^{24,25} to make movements that are potentially in conflict with task goals. Therefore, our initial hypothesis— that this nonlinearity would produce *increased* deviation from a Gaussian velocity distribution as sensory salience was *reduced*—was not supported. Our initial intuition failed because we did not appreciate that decreases in sensory salience drives the selection of explore behavior, and that behavior itself is approximately Gaussian, ultimately reducing the relative prominence of the task-oriented central peak.

Interestingly, reanalysis of data from a previous study of exploratory movements in a similar refuge tracking paradigm in *E. virescens* show the same relationship between sensory salience and changes in velocity profiles, but for modulations of a different sensory modality, namely electrosensation.³ In these previous experiments, artificially generated electrical signals were used to diminish the salience of electrosensory information as the electric fish performed the refuge tracking. Our reanalysis of these published data (see Supplementary Material and Methods for details) showed that fish exhibited the distinctive non-Gaussian distribution of velocities. Moreover, the velocity distributions were modulated in relation to electrosensory salience: lower kurtosis values (corresponding to more normal distributions) occurred in experimental trials with added artificial electrosensory "jamming" signals (Extended Data Fig. 2a–f).

Sensory salience drives explore—exploit mode switching

How do changes in sensory salience drive changes in mode switching? To investigate this question, we segregated the velocity trajectories into "S", a slow velocity mode (exploit) comprising task-oriented, station-keeping movements, and "F", a fast velocity mode (explore) comprising large positive (forward) and negative (backward) movement velocities (Fig. 2a,b, Extended Data Fig. 3, Supplementary Fig. 2) (see Methods for different clustering algorithms used).

Fish produced slow and fast velocity modes of movements in both lights-on and lights-off trials. We computed the residence time in each behavioral mode as a proportion of the total time spent in that mode compared to the trial duration of $40 \,\mathrm{s}$ (note that the residence time in slow and fast modes adds up to unity). The residence time τ_s

in the slow exploit mode was significantly higher (> 1.7 times) in lights-on trials than the lights-off trials (Fig. 2c). In contrast, the residence time in the fast explore mode $(1 - \tau_s)$ was higher in light-off than in lights-on trials.

Fish switched between slow and fast modes more frequently in lights-off trials than in lights-on trials (Fig. 2d). From the computation of the transition rates between slow (S) and fast (F) modes as a two-state Markov process, we found that the transition rate $S \to F$ was significantly lower in lights-on versus lights-off trials, i.e., the slow (exploit) state was visited more frequently in the lights-on trials compared to lights-off trials (Extended Data Fig. 3b). This salience-dependent modulation of switching frequency was the key mechanism by which movement velocity distributions trended toward a Gaussian distribution as a function of decreased sensory salience.

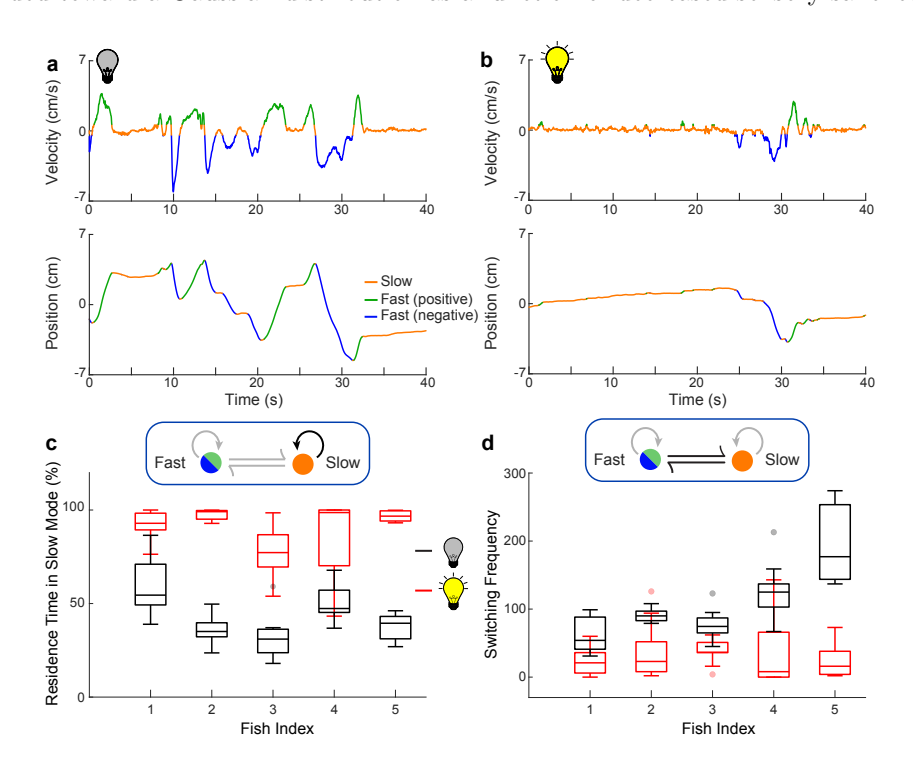


Fig. 2. Bursts of faster movements are more common in lights-off trials than in lights-on trials. (a,b) Fish showed two distinct behavioral modes, slow movement and fast movement, as seen in the velocity (top) and position traces (bottom) of representative trials from the same fish under lights-off (a) and lights-on (b) conditions. (c) The residence time in the slow mode, computed as the percent of the trial duration (40 s), was significantly higher during lights-on trials than lights-off trials (one-sided p-values are 0.0002, 0.0001, 0.0001, and 0.0001, respectively). (d) The switching between the fast mode (positive and negative combined) and slow mode was significantly more frequent in lights-off trials (black) than in lights-on trials (red) (one-sided p-value are 0.0037, 0.0070, 0.0008, 0.0045, and 0.0001, respectively). All box and whisker plots include the median line, the box denotes the interquartile range (IQR), whiskers denote the rest of the data distribution and outliers are denoted by points greater than $\pm 1.5 \times \text{IQR}$. For both (c,d), the p-values were calculated using the Mann-Whitney-Wilcoxon test. The total number of lights-off trials (n) for fish 1 and 3 was 7, and for the rest, it was 10 trials per condition per fish.

Mode-switching across taxa, behaviors, and sensory modalities

Is this mode-switching strategy solution for the explore versus exploit problem found in other species, in other categories of behavioral tasks, and in control systems that rely on other sensing modalities?

To answer this question we analyzed published data for an additional ten species, representing a wide phylogenetic range of taxa, from single-celled organisms to humans, involving categorically different tasks and sensorimotor regimes.^{3,14–20,22} These taxonomically diverse species were selected to encompass a wide range of behaviors that rely on a broad range of sensory systems (Fig. 3). For every example we examined, we found the same distinctive non-normal distribution of velocities, with a peak at low velocity movements and broad shoulders for higher velocity

movements (Fig. 4).

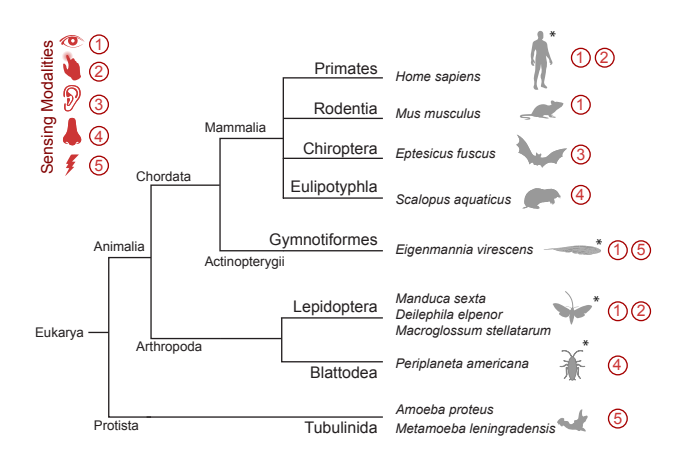


Fig. 3. Diversity of organisms and sensing modalities used for analysing mode-switching strategies. The major sensing modalities (vision, tactile sensing, audition, olfaction, and eletrosensation) used for task execution are listed next to the organisms (four species of mammals, a species of ray-finned fish, four species of insects, and two species of amoebae). The effect of sensory salience is studied for organisms marked with asterisks. Behaviors and movement statistics of the organisms are shown in greater detail in Fig. 4.

For example, postural sway movements in humans are thought to prevent the fading of postural state information during balance.²⁶ Our reanalysis of quiescent stance data¹⁷ revealed evidence of mode switching (Fig. 4a) that is remarkably similar to our findings in electric fish. In the quiescent stance task, human subjects used visual and tactile feedback to maintain an upright posture. The distribution of sway velocities revealed a distinct peak at low velocities corresponding to the task goal, and broad shoulders for higher velocities produced by the exploratory movements; the velocity statistics were better captured by a GMM than a normal distribution. Furthermore, the velocity distribution showed the same surprising relation to changes in salience, becoming more Gaussian as well as increase in the switching frequency when sensory salience was decreased (Extended Data Fig. 4a–d), as seen in the electric fish *E. virescens*.

Mode switching was also observed in invertebrate species. For example, the Carolina sphinx hawkmoth (Manduca sexta) uses somatosensory feedback from their proboscis to detect the curvature of flowers when searching for nectaries at dawn and dusk.²⁰ In this search behavior, which has dynamics that are qualitatively similar to vibrissal sensing in rats,²⁷ the moth sweeps its proboscis across the surface of the flower using a combination of slow- and high-velocity movements. Our analysis of the distribution of the rate of change of radial orientation angle (angle between the proboscis tip trajectory and the radial axis of the flower), before the insertion of the proboscis tip into the nectary shows the characteristic sharp peak with broad-shoulders (Fig. 4g) that is captured by a GMM. Experimental changes in the shape of artificial flowers that degrade the salience of the curvature of the flower surface²⁰ resulted in a decrease of the kurtosis value of the proboscis angular velocity distribution (Extended Data Fig. 5a–f), similar to how both E. virescens and humans responded to changes in sensory salience.

The fact that this salience-based, mode switching strategy was found in two distantly related classes (mammalia and insecta) performing very different behaviors, using different sensorimotor systems, suggests that the strategy emerged as a convergent solution to the explore versus exploit problem. We found additional evidence of convergence of this solution in reanalysis of eight additional datasets: visual saccades in humans (Fig. 4b, Supplementary Fig. 3)²¹ and in house mice *Mus musculus* (Fig. 3c, Supplementary Fig. 4),¹⁵ movements of the pinnae of echolocating big brown bats *Eptesicus fuscus* (Fig. 4d, Supplementary Fig. 5),¹⁶ olfaction in Eastern moles *Scalopus aquaticus* (Fig. 4e, Supplementary Fig. 6)¹⁴ and American cockroaches *Periplaneta americana* (Fig. 4f, Extended Data Fig. 4e–f),¹⁸ and visual tracking of a swaying flower in three species of hawkmoths (*Manduca sexta, Deilephila elpenor, Macroglossum stellatarum*) (Fig. 4h, Extended Data Fig. 5 g–p).¹⁹ The discovery of a similar, parsimonious velocity distributions across taxa, behavior, and sensing modalities, with consistent dependency on sensory salience, was surprising.

Intriguingly, our analysis of the dynamics of transverse exploration by pseudopods of amoebae²² (*Amoeba proteus* and *Metamoeba leningradensis*) reveals similar GMM velocity distributions in response to an electric field (Extended Data Fig. 6). Although our modeling approach (see next section) includes inertial dynamics, that cannot be directly

applied to movement of organisms in the low Reynolds number regimes occupied by single-celled and other microscopic organisms, these observations are consistent with a mode-switching strategy for the control of movement in these amoebae.

The examples described above include a broad phylogenetic array of organisms that perform a variety of behavioral tasks using different control and morphophysiological systems. Just as these behavioral systems evolved within each of the lineages represented in our reanalyses, we suggest that mode switching likely evolved independently in each lineage as well. In other words, the similarities we found across taxa are the result of convergent evolution towards a common solution—mode switching—for the explore versus exploit problem.

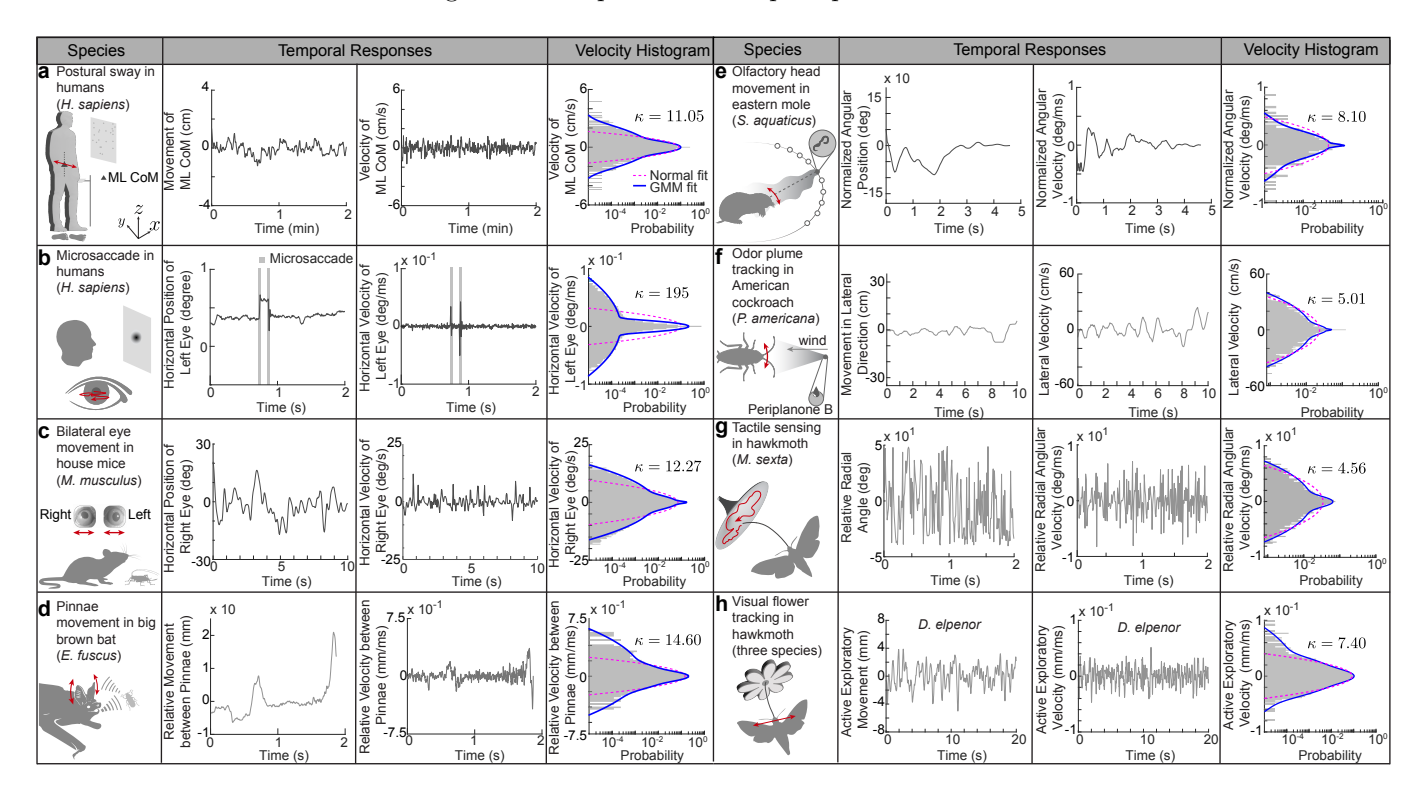


Fig. 4. Broad-shouldered velocity distribution is found across taxa, behaviors, and sensing modalities. Reanalysis of data from eight prior studies reveals a convergent statistical structure of movements across a range of organisms and behaviors: (a) postural sway in humans (Homo sapiens) during maintenance of quiet upright stance, ¹⁷ (b) microsaccades in humans (*Homo sapiens*) during fixated gaze, ²¹ (c) bilateral eye movements in mice (Mus musculus) during prey (cricket) capture, 15 (d) pinnae movements in big brown bats (Eptesicus fuscus) while echolocating prey (mealworm), ¹⁶ (e) olfactory driven head movements in eastern moles (Scalopus aquaticus) in response to food (earthworms), ¹⁴ (f) odor plume tracking in American cockroaches (Periplaneta americana) in response to sex pheromone (Periplanone B), 18 (g) tactile sensing by Carolina sphinx hawkmoth (Manduca sexta) while searching for a flower nectary, 20 and (h) visual tracking of swaying flower by hawkmoths 19 (three species; only data from elephant hawkmoth, Deilephila elpenor is shown, for the remainder see Extended Data Fig. 5g-p). The second column shows representative temporal traces of the active exploratory movements, the third column shows the respective velocity traces. The fourth column presents velocity histograms showing that, unlike the normal distribution (magenta dashed curve), the three-component Gaussian mixture model (GMM; blue solid curve) captures the broad-shouldered nature of the velocity data across species, behaviors, and sensing modalities. See Supplementary Materials and Methods for detailed method and Extended Data Table 2 for statistical details. Photo credit: Mice eye image courtesy of authors in Michaiel et al., 15 published under the terms of the Creative Commons Attribution License.

Heuristic model of the mode-switching strategy

Why might animals use mode switching, rather than the simpler heuristic of applying continual, low-amplitude exploratory inputs used by control engineers¹³? To address this question, we propose a parsimonious heuristic model

that comprises a nonlinear motion-dependent sensor, a linear musculoskeletal plant, a state estimator (also known as an observer²⁸), and a mode-switching controller (Fig. 5a). For the musculoskeletal plant, we assumed a simplified second-order Newtonian model:^{9,24}

$$\frac{dx(t)}{dt} = v(t),$$

$$\frac{dv(t)}{dt} = -\frac{b}{m}v(t) + \frac{1}{m}u(t) + w_1(t).$$
(1)

Here x(t) is dimensionless position, v(t) is dimensionless velocity, u(t) is the controller input, and $w_1(t)$ is process noise. The process noise includes noise due to physical disturbances^{29,30} as well as motor noise.³¹ The system parameters m and b represent unitless mass and viscous damping, respectively.

The key feature of the model is that the nonlinear sensory system (i.e. "motion dependent sensor") embodies the high-pass filtering (i.e., fading or adapting) characteristics found across biological sensory systems.^{26,32–38} This sensory system model ("motion dependent sensor" in Fig. 5a) assumes nonlinear measurements that decay to zero over time in the face of constant stimuli:

$$y(t) = \frac{d}{dt}s(x(t)) + w_2(t) = g(x)v(t) + w_2(t).$$
(2)

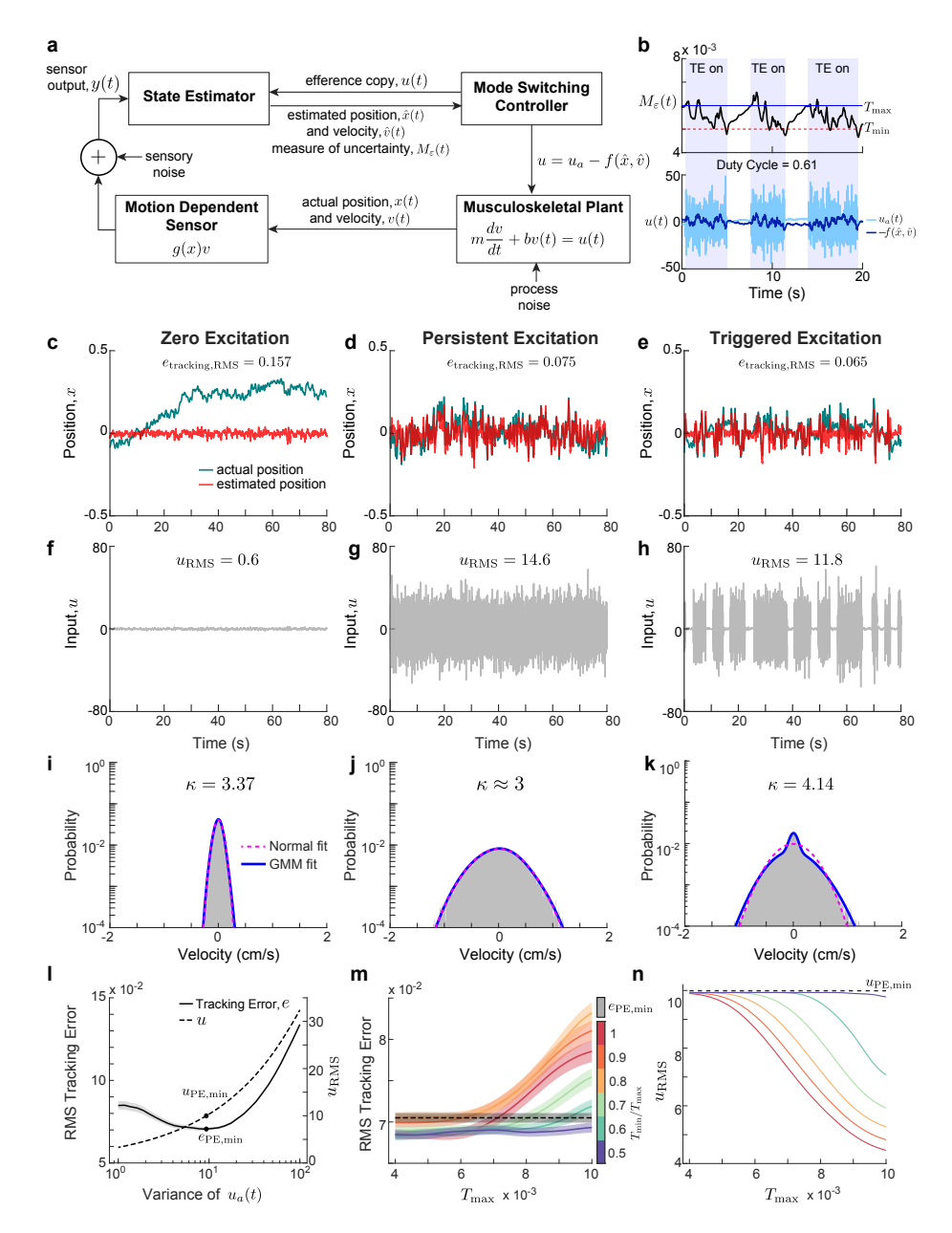
Here, s(x) is the position dependent sensory stimulus experienced by the organism, g(x) is the spatial derivative of the sensory stimulus (ds(x)/dx), and $w_2(t)$ is the sensory noise. The controller includes a state-feedback-based task level control policy, $-f(\hat{x},\hat{v})$, that exploits previously collected sensory information; that information is parsimoniously encoded (i) in estimates of the position and velocity (\hat{x},\hat{v}) , and (ii) in an ongoing measure of uncertainty, M_{ε} (based on the covariance of position and velocity estimates). Previous theoretical work has demonstrated that exploratory movements are required for state estimation in control systems that rely on such high pass (i.e., fading) sensors. ^{24, 25} Hence, the controller also includes an active sensing control policy, $u_a(t)$, that seeks to gain new information through exploratory movements.

To find the optimal balance between exploit and explore components, for a given admissible control policy, π and a given weight, r for an input, $u \in \mathcal{U}$ (action space), we can define the average steady state cost function:

$$J_{\pi} = \limsup_{t \to \infty} \mathbb{E}[x(t)^2 + ru(t)^2] \tag{3}$$

where $\mathbb E$ is the expectation computed over all the trajectories induced by admissible control policy, π . Note that a control policy is admissible if it depends causally on the sensor and actuator data. We chose the cost function, J_{π} as a weighted combination of steady state tracking error and control effort. Even with complete knowledge of the system states, computation of the optimal solution $J_{\pi^*} = \inf_{\pi \in \Pi} J_{\pi}$ where Π is the set of all admissible control policies, is only tractable in the case of linear systems or systems with finite state and action spaces.³⁹ Since the system is partially observed, existing approaches to optimal control require the solution to an optimal filtering problem and then formulate feedback laws on the filter states.³⁹ The filtering problem requires computation of the conditional probability $\mathbb{P}\left(\begin{bmatrix} x(t) \\ v(t) \end{bmatrix} \mid y(\tau), u(\tau) \, \forall \tau \leq t \right)$. However, due to nonlinearity in the measurement (Eqn. (2)), there is no tractable method to compute this conditional probability, and so heuristic strategies are required. We tested three exploratory movement heuristics for the controller to find an approximate answer to this intractable optimal control problem:

- 1. **Zero Excitation:** This is a passive strategy (i.e., no exploration) in which the system provides no input excitation for the actuation forces $(u_a(t) = 0 \text{ for all } t)$. This is a conventional state-feedback controller.
- 2. **Persistent Excitation:** This scheme tests a common continuous exploration strategy used in the field of adaptive control.¹³ The controller continually injects a Gaussian input $u_a(t)$.
- 3. **Triggered Excitation:** This mode-switching strategy depends on lower and upper thresholds, T_{\min} and T_{\max} ; the controller only injects Gaussian input when the uncertainty in the state estimator M_{ε} exceeds T_{\max} , and then continues to inject input until this uncertainty drops below a lower threshold, T_{\min} (Fig. 5b).



Template model illustrating three different exploration strategies. (a) Schematic of the Triggered Excitation (mode-switching) strategy. The musculoskeletal plant for animal locomotion has two statesposition (x) and velocity (v). The state estimator has access to noisy measurements from a nonlinear adaptive sensor (g(x)v). The state estimator (extended Kalman filter) is designed to work in tandem with the mode switching controller. The controller output, u comprises both state-feedback $(-f(\hat{x},\hat{v}))$ and an active sensing component $(u_a(t))$. See Methods for details. (b) Triggered Excitation (TE) strategy showing the temporal traces of measure of uncertainty (M_{ε} , trace of the error covariance) with threshold levels $T_{\min} = 4.8 \times 10^{-3}$ and $T_{\text{max}} = 6 \times 10^{-3}$ (top), input u (bottom; active sensing component, $u_a(t)$: light blue; state-feedback component, $-f(\hat{x},\hat{v})$: dark blue). The triggering started as M_{ε} exceeded T_{\max} and the triggering continued till M_{ε} dropped below T_{min}. (c-e) Simulated position traces (actual states: teal, estimated states: red) using three different exploratory movement strategies for $u_a(t)$: Zero Excitation (c), Persistent Excitation (d), and Triggered Excitation (e) along with the state-feedback. The respective RMS values of the tracking error (e_{RMS}) are shown in the panels. (f-k) Controller input traces (f-h) and velocity histograms (i-k) for various schemes as in (c-e). Respective RMS values of the inputs (u_{RMS}) are shown in the panels of (f-h). In (i-k) the fits with a normal distribution (magenta dashed) and three-component Gaussian mixture model (blue solid) are shown along with the respective kurtosis (κ) values. (1) Effect of exploratory movement (variance of $u_a(t)$) on tracking error (e) and control effort (u) in Persistent Excitation (PE). The minimum RMS tracking error and the corresponding control effort are denoted as $e_{\mathrm{PE,min}}$ and $u_{\mathrm{PE,min}}$, respectively. (m,n) Effect of threshold pair ($T_{\mathrm{max}}, T_{\mathrm{min}}$) in Triggered Excitation on tracking error (m) and control effort (n) at optimum variance of $u_a(t)$ corresponds to $e_{PE,min}$. The solid lines in (m,n) show the respective mean and the shaded regions in (m) correspond to respective SEM (n = 300 independent simulations). Note that with the right choice of threshold pair, Triggered Excitation scheme can achieve lower tracking error with substantially lower control effort.

As prior theoretical work shows, 25 the Zero Excitation strategy (i.e., traditional state-estimate feedback) cannot minimize the state estimation error and hence, not surprisingly, results in poor tracking performance (Fig. 5c), thus illustrating the need for an additional active sensing component in the face of adaptive sensing and perceptual fading. The Persistent Excitation and Triggered Excitation strategies both facilitate substantially better position control than does the Zero Excitation strategy (Fig. 5c,d). Though these two strategies resulted in comparable tracking errors ($e_{\rm RMS}$, Fig. 5b,c), the Triggered Excitation was more efficient, requiring substantially lower control effort ($u_{\rm RMS}$, Fig. 5g,h). Moreover, unlike the Persistent Excitation strategy, Triggered Excitation generated a distinctive broadshouldered velocity distribution that featured a sharp peak near zero, with broad shoulders corresponding to bursts of fast movement (Fig. 5j,k). This distribution was strikingly similar to experimental observations across organisms (Fig. 1, Fig. 4, Extended Data Fig. 4, Extended Data Fig. 5, Extended Data Fig. 6), suggesting that such broad shoulders are a signature (if not definitive proof) of a mode-switching strategy.

We showed that active exploration is essential for better tracking performance as it improves state estimation. But, there is a point of diminishing returns: although higher (more energetic) active excitation can result in excellent state estimation, there is a point beyond which these additional active sensing movements lead to greater tracking errors.

To contrast between Persistent and Triggered Excitation we performed a numerical study to obtain the variance of the active sensing signal $u_a(t)$ that minimizes RMS tracking error for the Persistent Excitation (PE) strategy, $e_{\text{PE,min}}$. Note that Persistent Excitation is the limiting case of Triggered Excitation with extremely low threshold values (i.e., insuring that the active sensing mode is always "on"). With that optimum stimulation obtained from Persistent Excitation, we next performed a parameter sweep involving threshold pair $(T_{\text{max}}, T_{\text{min}})$ in the Triggered Excitation. We discovered that the choice of thresholds in the Triggered Excitation strategy plays an important role—with the right choice of parameters we could achieve better tracking performance (Fig. 5m) at reduced control effort (Fig. 5n). The choice of thresholds also shapes the velocity to best extract sensory information; with low thresholds, the statistics approach that of the Persistent Excitation, whereas high thresholds lead to velocity distributions with higher kurtosis (departure from normality), while requiring less control effort (Extended Data Fig. 7a–c).

How does sensory salience affect performance of the Triggered Excitation (mode-switching) heuristic? To simulate the effects of changes in sensory salience, we parametrically varied the sensory noise variance while keeping constant the switching thresholds T_{\min} and T_{\max} . As the sensory noise variance was increased (simulating a decrease in salience), the kurtosis value of the velocity distribution decreased, numerically approaching normality in the limit of high sensory noise (Extended Data Fig. 7d–g). This trend of decreased kurtosis in the face of increased noise variance captures the widespread observation that in animals the velocity statistics tend toward a Gaussian distribution as sensory salience is decreased. Moreover, the underlying mechanism, namely increasing frequency of bursts of exploratory movements, matches our experimental observations in E. virescens, which performed more frequent transitions to fast movements and spent less time in the slow mode in the lights-off trials than in the lights-on trials (Fig. 2c,d). These analyses clarify that this trend toward a Gaussian distribution with decreased salience is an epiphenomenon of mode-switching: as the frequency of fast movement bursts increases, it overwhelms the task-oriented movements, diminishing the prominence of the central peak.

Discussion

We examined explore—exploit tradeoffs in the context of goal-direct motor behaviors, such as station keeping, postural balance, and plume tracking, that require active, exploratory movements to enhance sensation. We discovered that the velocity distributions that emerge from the interplay between exploratory movements and goal-directed control are broad-shouldered across taxa, and that this distinctive distribution of movements is robustly modulated by sensory salience. The bouts of ancillary movements that comprise the broad shoulders of these velocity distributions are commonly described as "active sensing", i.e., the expenditure of energy by organisms for the purpose of sensing, ⁴⁰ for example, ancillary movements described here. Active sensing also includes the emission of energetically costly signals such as electric fields by weakly electric fishes ⁴¹ and echolocation calls in dolphins, birds, and bats. ^{42–45} Active sensing research in humans, in relation to touch, was popularized in the 1960's by J.J. Gibson, ¹ and the original ideas date back at least to the 18th century (for a historical account, see Zweifel et al. ⁴⁰).

Surprisingly, active sensing is largely avoided in engineering design despite being ubiquitous in animals. The performance of engineered systems may benefit from the generation of movement for improved sensing. An algorithm known as Ergodic Information Harvesting (EIH)³ could be used to control movements for sensing in artificial systems.

This algorithm balances the energetic costs of generating movements against the expected reduction in sensory entropy. The EIH has been tested in relation to several animal model systems, and produces plausible animal trajectories.³

Interestingly, the EIH algorithm produces the opposite trend in kurtosis of velocity distributions in relation to sensory salience (Extended Data Fig. 2g–l, Extended Data Table. 3) that we observed in our experiments, reanalysis of prior data, and in our model: as sensory salience decreases, there is an increase in active sensing movements but a decrease in kurtosis (Extended Data Table. 2). That EIH leads to decrease in kurtosis occurs in part because EIH generates continuous sensing movements, and does not incorporate mode switching. A refined EIH model, that generates the temporally distinct periods of sensing movements that characterize mode switching, would better reflect our findings in animals, and is a promising strategy for improving the performance of robotic control systems.

How mode switching is manifest across the diverse biological systems we examined is a compelling open question. Many of these control systems have evolved via convergent evolution in which adaptive strategies emerge independently across lineages. One result of convergent adaptation is that species often rely on idiosyncratic features, such as feathers or skin flaps, to achieve the same adaptive strategy, such as flapping flight. We infer that the mechanisms for mode switching is present in control systems that range from sub-cellular systems 46 to neural systems in vertebrates.

The mechanisms for mode switching in vertebrate nervous systems may emerge at different levels within sensorimotor control pathways. For example, neurophysiological recordings show that sensory salience can be encoded in brain circuits via synchronization and desynchronization of spiking activity.⁴⁷ Such population coding of salience, when coupled with a threshold, could trigger discrete bursts of motor activity for sensing.⁸ Motor circuits for the production of discrete bursts of movement occur in spinal circuits.⁵¹

These discrete bursts of movements could arise from reflex-like, threshold-based activity in animals, akin to how Mauthner cells trigger a cascade of motor activity when sensory inputs exceed a threshold.⁵² A key difference between reflex-like, threshold-based behaviors and the mode-switching we describe in this paper would be that the signal in question would arise from an internal representation of sensory uncertainty, rather than from the overall level of sensory excitation. Such a reflex-like action could produce stereotyped forms of interactions with the external environment in relation to sensing.⁸

A common engineering approach to sensing and control is to add sensors and improve sensor performance, particularly at low frequencies, effectively side-stepping the need for active sensing movements altogether. Such improved sensing enhances observability without relying on movement. In stark contrast, organismal sensor systems are almost invariably adapting (high-pass), necessitating active sensing. Irrespective of whether organisms have achieved an optimal solution to the control problem (or instead are limited by evolutionary constraints on sensor performance), the widespread convergent evolution of a common active sensing strategy nevertheless suggests an alternate engineering design paradigm. The confluence of adapting sensors⁵³ and the uncertainty-triggered modeswitching heuristic presented in this paper provides a new roadmap for movement control of robotic systems.

In this paper, the explore–exploit tradeoff arises from the need for active state estimation²⁸ in a subset of tasks in which movement is used both for acquisition of information and achieving task goals. However, similar tradeoffs arise in a wide variety of potentially more complex behaviors. For example, in foraging where the resources are found in patchy distributions, organisms balance the tradeoffs between exploiting a local food source, exploring for distant sources,⁵⁴ and the costs of predation across the habitat.⁵⁵ Similarly, reinforcement learning involves choosing whether to adhere to a familiar option with a known reward or taking the risk to explore unknown options that can lead to increased rewards over the longer term.⁵⁶ We do not have direct evidence that the broad-shouldered feature we have identified in animal movements described here (Fig. 1, Fig. 4)—reflecting the manifestation of mode switching—are also found in these behavioral domains across taxa. Recent evidence from studies of human reinforcement learning, however, appear to be consistent with mode-switching behavior.

Methods

Tracking of glass knifefish

Subjects

We obtained adult, weakly electric, glass knifefish $Eigenmannia\ virescens\ (10-15\ cm$ in length) from commercial vendors, and housed the fish according to the published guidelines. ⁵⁷ Water temperature in the experimental tank was kept between $24-27\ ^{\circ}$ C, and conductivity ranged from $10-150\ \mu\text{S/cm}$. Fishes were transferred from the holding tank to the experimental tank 12-24 hours prior to the experiments, to allow for acclimation. All experimental procedures were approved by the Johns Hopkins Animal Care and Use Committee, and followed guidelines established by the National Research Council and the Society for Neuroscience.

Experimental apparatus

The experimental apparatus was similar to that used in previous studies. 2,6,8,23,58 The refuge was machined from a 152 mm long segment of 46×50 mm rectangular PVC tubing, with the bottom surface removed to allow the camera to record the ventral view of the fish. On both sides of the refuge, a series of six rectangular windows (6 mm wide \times 31 mm high, spaced 19 mm apart) were machined, through which to provide visual and electrosensory cues.

A computer sent designed digitized input stimuli (25 Hz) from LabVIEW (National Instruments, Austin, TX, USA) to a FPGA based controller for a stepper motor (STS-0620-R, HW W Technologies, Inc., Valencia, CA, USA). The stepper motor drove a linear actuator, leading to the one degree of freedom refuge movement in real time. A video camera (pco.1200, PCO AG, Kelheim, Germany) captured fish movements through mirror reflection at 100 Hz. The captured frames (width × height: 1280 pixels × 276 pixels) were saved as 16 bits .tif files via camera application software (pco.camware, PCO AG, Kelheim, Germany).

Experimental procedure

The experiments were conducted in two illuminance levels—around 0.3 lx (lights off) and 80 lx (lights on). Each trial lasted for 60 s. During the initial 10 s of each trial, the refuge was actuated to follow a 0.45 Hz sinusoidal trajectory, the amplitude of which was gradually increased to 3 cm, and then decreased to 0 at the end of the 10 s interval, in a similar fashion as described in Biswas $et~al.^2$ After the initiation phase, the refuge remained stationary for 40 s, finally followed by a termination phase for 10 s, during which the refuge was actuated in a similar fashion as during the initiation phase.

Tracking Algorithm

To observe fine details of the fish movement, we used a high frame rate in our video recordings. High tracking accuracy was essential as the position and velocity data were likely to be contaminated by measurement noise. To ensure high tracking accuracy, the refuge and fish position were analyzed by custom video tracking software ⁵⁹ developed by Balázs P. Vágvölgyi from the Laboratory for Computational Sensing and Robotics (LCSR), at Johns Hopkins University.

The tracking algorithm worked in two phases. The first phase was template matching, which roughly located the targets (fish or refuge). In the first frame of a given video, a rectangular region was manually selected around the target to create a template. On subsequent frames, a neighborhood region around the template (\pm 20 pixels) from the previous frame was selected for the computation of a normalized 2-D cross-correlation matrix. If the target changed its orientation in the new frames, before computing the normalized 2-D cross-correlation, the new image frame was first rotated to match the orientation of the template from previous frame. If needed, the areas of the image were sampled (then scaled and interpolated if necessary) with subpixel accuracy.

After creating the template, the second phase applied the Levenberg-Marquardt algorithm to find the global maximum of the normalized cross-correlation function. This step produced a match between the template and target at each frame, with subpixel accuracy. We performed extensive preliminary testing and analysis to confirm that the remaining measurement errors had smaller variance than the stochastic movements of the fish.

Data Processing

The tracking algorithm stored the fish position in both horizontal and vertical directions, (originally in pixels, along with the respective pixel to meter conversion factor), and the angle of orientation (in degree) in .csv files. We used only the data while the refuge was stationary (40 s, 4000 data points in total) for each trial. To further reduce the measurement noise, the position data was filtered through a Butterworth zero-phase distortion filter (filtfilt command in MATLAB) with a 10 Hz cutoff frequency. Fish velocity in the horizontal direction was computed as forward differences of the horizontal position time series.

Identification and Characterization of Behavioral Modes

For the identification of the behavioral modes, we used three different clustering approaches—(1) Gaussian mixture model (GMM) with inflection point based clustering, (2) hidden Markov model (HMM) based clustering, and (3) GMM with maximum a posteriori probability (MAP) based clustering.

For GMM with inflection point based clustering, the velocity (v) data from each individual fish at a specific lighting condition were clustered into three components, slow, fast positive, and fast negative (Extended Data Fig. 3a,b), using two velocity thresholds, v_L and v_H ($v_L < v_H$), resulting in two behavioral modes—slow and fast (fast positive and negative were combined). The velocity threshold values were computed by finding the inflection points of the GMM fits to the velocity data, $f_{\rm GMM}$, specific to a lighting condition. To numerically identify the inflection points of $f_{\rm GMM}$, we numerically computed the spatial second-order derivative of $f_{\rm GMM}$ ($f_{\rm GMM}''$), and located the first and the last indices of the array $\frac{f_{\rm GMM}''}{f_{\rm GMM}}$ such that the condition $\frac{f_{\rm GMM}''}{f_{\rm GMM}} < c$ was satisfied for a given c. This method separated the central peak of the $f_{\rm GMM}$, velocity distribution around zero velocity, from the broad shoulders. We chose c=0.005 for all the individual fish irrespective of the lighting conditions, except for fish 1 lights-off trials (c=0.02), (the different c value for fish 1 lights-off trials was chosen so that the relative area under the central peak of the distribution was less than 0.6 (similar to other fish during lights-off trials). For further analysis of these behavioral modes, we assumed a continuous time Markov chain model (Extended Data Fig. 3c,d). For infinitesimal dt, the transition probabilities, Q_{ij} are given as follows:

$$Pr(v(t+dt) = j|v(t) = i) = Q_{ij}dt + o(dt), \quad i \neq j$$
(4a)

$$Q_{ii} = -\sum_{i \neq j} Q_{ij} \tag{4b}$$

and the probability matrix \mathbf{P} with $p_{ij} = \Pr(v(t) = j | v(0) = i)$ and transition rate matrix \mathbf{Q} with entries Q_{ij} satisfy the first order differential equation

$$\frac{d}{dt}\mathbf{P} = \mathbf{PQ},\tag{5}$$

whose solution is given by,

$$\mathbf{P} = e^{t\mathbf{Q}} = \sum_{n=0}^{\infty} \frac{(tQ)^n}{n!}.$$
 (6)

For every trial from each individual fish, we computed the probability matrix \mathbf{P} with entries p_{ij} , i=1,2,j=1,2 where state 1 and 2 correspond to slow (exploit) and fast (explore) modes, respectively. We used the approximation to the matrix exponential in Eqn. (6), $\mathbf{Q} \approx \frac{1}{h}(\mathbf{P} - I)$ for the computation of the transition rates between slow and fast modes in each trial from the respective probability matrix, \mathbf{P} .

For HMM clustering, we combined all the positional trial data (x_t) from all the five fish at a specific lighting condition along with their negatives $(-x_t)$. (We included the negative data to eliminate any directional bias.) We assumed that the observed measurements of position, x_t , follow a homogeneous Markov switching first-order autoregressive model:

$$x_t = \alpha_0^{s_t} + \alpha_1^{s_t} x_{t-1} + \sigma \varepsilon_t \tag{7}$$

where the superscript $s_t \in \{1, 2, 3\}$ refers to the hidden discrete state and ε is Gaussian white noise. We fit this model using the NHMSAR package in R.

The HMM fitting resulted in three clusters similar to slow, fast positive, and fast negative as obtained with GMM with inflection point based clustering method (Extended Data Fig. 3e–h). Finally by combining fast positive and

negative, we ended up with two behavioral modes—fast and slow for further computation of switching frequency and residence time.

In GMM with MAP based clustering, GMM models with three components were fitted to the velocity data from each individual fish at a specific lighting condition. We assigned the cluster index for each data point based on the maximum a posteriori probability using Bayes' rule. This method required a *post hoc* assignment of which cluster or clusters correspond to the "slow" behavioral mode in order to compute residence time; see for example Extended Data Fig. 3i–m.

All analysis was performed using code written in R and MATLAB.

Gaussian noise inputs with variances 0.03 and 10, respectively.

Simulation

Sensory adaptation is a robustly observed phenomenon among organisms ranging from unicellular amoebae^{37,38} to humans²⁶ where the sensory systems stop responding to constant stimuli. Here, we modeled this adaptive/high-pass nature of the sensory receptors as a "motion dependent sensor" for which we assumed a nonlinear measurement model^{24,25} with sensory noise $w_2(t)$:

$$y(t) = \frac{d}{dt}s(x(t)) + w_2(t) = \frac{d}{dx}s(x(t))v(t) + w_2(t) = g(x)v(t) + w_2(t).$$
(8)

Here, s(x) is the position dependent sensory scene experienced by the organism. For the present study, we assumed a quadratic sensory scene $s(x) = \frac{1}{2}\alpha x^2 + \beta x$ with nonzero constant sensory scene parameters α and β . This assumption on sensory scene yields $g(x) = \alpha x + \beta$, a linear function of position, x.

Due to the presence of the nonlinearity in the measurement, we used an extended Kalman filter (EKF) for state estimation, a common heuristic. For the state-feedback component we applied $f(\hat{x}, \hat{v}) = k_1 \hat{x} + k_2 \hat{v}$. In the Triggered Excitation scheme, for the uncertainty measure (M_{ε}) we used the trace of the state estimation error covariance matrix, Tr(P(t)). When the uncertainty measure Tr(P(t)) rose above a maximum threshold, T_{max} , the controller generated active sensing component, $u_a(t)$ as a Gaussian input with fixed power spectral density and it continued to inject the input until Tr(P(t)) dropped below a lower threshold, T_{min} . At this point the controller switched back to traditional state-feedback form. For the Persistent Excitation scheme, the controller continued to inject a Gaussian input $u_a(t)$ for all time.

To obtain the critical excitation level of the active sensing component $u_{a,\text{crit}}(t)$ for optimum tracking performance in Persistent Excitation, we chose 30 logarithmically spaced variance values of $u_a(t)$ from 1 to 100. From the mean of 100 independent simulations for each variance value, we obtained $u_{a,\text{crit}}(t) \approx 9.33$ which achieved the minimum RMS tracking error of $e_{\text{PE,min}} \approx 0.071$ and RMS control effort $u_{\text{PE}} \approx 10$. Using this critical value for the excitation $u_{a,\text{crit}}(t)$, we studied the effect of thresholds in Triggered Excitation by varying T_{max} and $T_{\text{max}}/T_{\text{min}}$ linearly from 4×10^{-3} to 10×10^{-3} , and 0.5 to 1, respectively, and performed 300 independent simulations for each pair of values. The system parameters were chosen from prior studies^{6,24} as follows: b = 1.7, m = 1, $\alpha = 3$, $\beta = 5$, $k_1 = m\omega_n^2$, $k_2 = (2m\zeta\omega_n + b)$, $\zeta = 0.56$, $\omega_n = 1.05 \times 2\pi$. The process noise, $w_1(t)$ and sensor noise, $w_2(t)$ were chosen as fixed

Statistics

All the statistical analysis was performed with sign test and Mann-Whitney-Wilcoxon test using custom codes written in R (R core team, Indianapolis, Indiana, USA) and MATLAB (Mathworks, Natick, Massachusetts, USA). For all tests, the significance level was set to 0.05. The experimental and simulation data are provided as either mean plus or minus the standard deviation ($\mu\pm SD$) or mean plus or minus the standard error of the mean ($\mu\pm SD$).

Data availability

An archived version of the datasets supporting this article is available through the Johns Hopkins University Data Archive with the following DOI: $https://doi.org/10.7281/T1/QS3QFT^{60}$

Code availability

An archived version of the analysis codes supporting this article is available through the Johns Hopkins University Data Archive with the following https://doi.org/10.7281/T1/QS3QFT⁶⁰

Acknowledgement

We thank Tim Kiemel (UMD) for providing human balance data and Balázs P. Vágvölgyi (JHU) for developing the tracking software used in this work. We thank Cynthia F. Moss (JHU), Varun P. Sharma (GT) and Simon Sponberg (GT) for suggesting relevant articles for the reanalysis of the animal locomotion data, and Sarah L. Poynton (JHMI) for critical feedback on the manuscript. This work was supported by the Office of Naval Research under grant no. N00014-21-1-2431 (N.J.C) and the National Science Foundation under grant no. 2011619 (N.J.C.).

Author contribution

Conceptualization, all authors; Methodology, all authors; Software, D.B., A.L., K.H., Y.Y. and J.G.; Formal Analysis, D.B., A.L., K.H., Y.Y. and J.G.; Investigation, Y.Y.; Data Curation, D.B. and Y.Y.; Writing – Original Draft, all authors; Writing – Review and Editing, all authors; Visualization, D.B. with other authors; Supervision, N.J.C.

Declaration of Interests

The authors declare no competing interests.

References

- [1] Gibson, J. J. Observations on active touch. Psychol Rev 69, 477–491 (1962).
- [2] Biswas, D. et al. Closed-loop control of active sensing movements regulates sensory slip. Curr Biol 28, 4029–4036 (2018).
- [3] Chen, C., Murphey, T. D. & MacIver, M. A. Tuning movement for sensing in an uncertain world. eLife 9, e52371 (2020).
- [4] Soatto, S. Actionable information in vision. In Machine learning for computer vision, 17–48 (Springer, 2013).
- [5] Stamper, S. A., Roth, E., Cowan, N. J. & Fortune, E. S. Active sensing via movement shapes spatiotemporal patterns of sensory feedback. *J Exp Biol* **215**, 1567–1574 (2012).
- [6] Cowan, N. J. & Fortune, E. S. The critical role of locomotion mechanics in decoding sensory systems. J Neurosci 27, 1123–1128 (2007).
- [7] Rose, G. J. & Canfield, J. G. Longitudinal tracking responses of the weakly electric fish, Sternopygus. J Comp Physiol A 171, 791–798 (1993).
- [8] Uyanik, I., Stamper, S. A., Cowan, N. J. & Fortune, E. S. Sensory cues modulate smooth pursuit and active sensing movements. Front Behav Neurosci 13, 59 (2019).
- [9] Sefati, S. et al. Mutually opposing forces during locomotion can eliminate the tradeoff between maneuverability and stability. Proc Natl Acad Sci U.S.A. 110, 18798–18803 (2013).
- [10] Golovin, D. & Krause, A. Adaptive submodularity: Theory and applications in active learning and stochastic optimization. *J Artif Intell Res* **42**, 427–486 (2011).
- [11] Cooper, G. F. The computational complexity of probabilistic inference using Bayesian belief networks. *Artif Intell* 42, 393–405 (1990).
- [12] Blondel, V. D. & Tsitsiklis, J. N. A survey of computational complexity results in systems and control. Automatica 36, 1249–1274 (2000).
- [13] Narendra, K. S. & Annaswamy, A. M. Persistent excitation in adaptive systems. Int J Control 45, 127–160 (1987).
- [14] Catania, K. C. Stereo and serial sniffing guide navigation to an odour source in a mammal. *Nat Commun* 4, 1–8 (2013).
- [15] Michaiel, A. M., Abe, E. T. & Niell, C. M. Dynamics of gaze control during prey capture in freely moving mice. eLife 9, e57458 (2020).
- [16] Wohlgemuth, M. J., Kothari, N. B. & Moss, C. F. Action enhances acoustic cues for 3-D target localization by echolocating bats. *PLoS Biol* 14, e1002544 (2016).
- [17] Kiemel, T., Oie, K. S. & Jeka, J. J. Multisensory fusion and the stochastic structure of postural sway. *Biol Cybern* 87, 262–277 (2002).
- [18] Lockey, J. K. & Willis, M. A. One antenna, two antennae, big antennae, small: total antennae length, not bilateral symmetry, predicts odor-tracking performance in the American cockroach *Periplaneta americana*. J Exp Biol 218, 2156–2165 (2015).
- [19] Stöckl, A. L., Kihlström, K., Chandler, S. & Sponberg, S. Comparative system identification of flower tracking performance in three hawkmoth species reveals adaptations for dim light vision. *Philos Trans R Soc Lond B Biol Sci* 372, 20160078 (2017).
- [20] Deora, T., Ahmed, M. A., Daniel, T. L. & Brunton, B. W. Tactile active sensing in an insect plant pollinator. J Exp Biol 224, jeb239442 (2021).

- [21] Hauperich, A.-K., Young, L. K. & Smithson, H. E. What makes a microsaccade? A review of 70 years of research prompts a new detection method. *J Eye Mov Res* **12** (2019).
- [22] De la Fuente, I. M. et al. Evidence of conditioned behavior in amoebae. Nat Commun 10, 1–12 (2019).
- [23] Sutton, E. E., Demir, A., Stamper, S. A., Fortune, E. S. & Cowan, N. J. Dynamic modulation of visual and electrosensory gains for locomotor control. *J R Soc Interface* **13**, 20160057 (2016).
- [24] Kunapareddy, A. & Cowan, N. J. Recovering observability via active sensing. In *Proc Amer Control Conf*, 2821–2826 (IEEE, Milwaukee, WI, USA, 2018).
- [25] Sontag, E. D., Biswas, D. & Cowan, N. J. An observability result related to active sensing (2022). URL https://arxiv.org/abs/2210.03848.
- [26] Fabre, M. et al. Large postural sways prevent foot tactile information from fading: Neurophysiological evidence. Cereb Cortex Comm 2 (2020).
- [27] Arkley, K., Grant, R. A., Mitchinson, B. & Prescott, T. J. Strategy change in vibrissal active sensing during rat locomotion. *Curr Biol* **24**, 1507–1512 (2014).
- [28] Yang, S. C.-H., Wolpert, D. M. & Lengyel, M. Theoretical perspectives on active sensing. *Curr Opin Behav Sci* 11, 100–108 (2016).
- [29] Matthews, M. & Sponberg, S. Hawkmoth flight in the unsteady wakes of flowers. J Exp Biol 221, jeb179259 (2018).
- [30] Tritico, H. M. & Cotel, A. J. The effects of turbulent eddies on the stability and critical swimming speed of creek chub Semotilus atromaculatus. J Exp Biol 213, 2284–2293 (2010).
- [31] Harris, C. M. & Wolpert, D. M. Signal-dependent noise determines motor planning. *Nature* **394**, 780–784 (1998).
- [32] Nelson, M., Xu, Z. & Payne, J. Characterization and modeling of p-type electrosensory afferent responses to amplitude modulations in a wave-type electric fish. *J Comp Physiol A* **181**, 532–544 (1997).
- [33] Lee, J. et al. Templates and anchors for antenna-based wall following in cockroaches and robots. *IEEE Trans Robot* 24, 130–143 (2008).
- [34] Jun, J. J., Longtin, A. & Maler, L. Active sensing associated with spatial learning reveals memory-based attention in an electric fish. *J Neurophysiol* 115, 2577–2592 (2016).
- [35] Clarke, S. E., Naud, R., Longtin, A. & Maler, L. Speed-invariant encoding of looming object distance requires power law spike rate adaptation. *Proc Natl Acad Sci U.S.A.* **110**, 13624–13629 (2013).
- [36] Clarke, S. E., Longtin, A. & Maler, L. A neural code for looming and receding motion is distributed over a population of electrosensory on and off contrast cells. *Journal of Neuroscience* **34**, 5583–5594 (2014).
- [37] Takeda, K. et al. Incoherent feedforward control governs adaptation of activated ras in a eukaryotic chemotaxis pathway. Science signaling 5, ra2–ra2 (2012).
- [38] Biswas, D., Devreotes, P. N. & Iglesias, P. A. Three-dimensional stochastic simulation of chemoattractant-mediated excitability in cells. PLoS Comput Biol 17, e1008803 (2021).
- [39] Bertsekas, D. Dynamic programming and optimal control: Volume I, vol. 1 (Athena scientific, 2012).
- [40] Zweifel, N. O. & Hartmann, M. J. Defining "active sensing" through an analysis of sensing energetics: homeoactive and alloactive sensing. *J Neurophys* **124**, 40–48 (2020).
- [41] Bullock, T. H. Electroreception. Annu Rev Neurosci 5, 121–170 (1982).
- [42] Brinkløv, S., Elemans, C. P. & Ratcliffe, J. M. Oilbirds produce echolocation signals beyond their best hearing range and adjust signal design to natural light conditions. R Soc Open Sci 4, 170255 (2017).

- [43] Nelson, M. E. & MacIver, M. A. Sensory acquisition in active sensing systems. *J Comp Physiol A* **192**, 573–586 (2006).
- [44] Snyder, J. B., Nelson, M. E., Burdick, J. W. & MacIver, M. A. Omnidirectional sensory and motor volumes in electric fish. *PLoS Biol* 5, e301 (2007).
- [45] Ghose, K. & Moss, C. F. Steering by hearing: a bat's acoustic gaze is linked to its flight motor output by a delayed, adaptive linear law. *J Neurosci* **26**, 1704–1710 (2006).
- [46] Berg, H. C. & Brown, D. A. Chemotaxis in *Escherichia coli* analysed by three-dimensional tracking. *Nature* 239, 500–504 (1972).
- [47] Benda, J., Longtin, A. & Maler, L. A synchronization-desynchronization code for natural communication signals. Neuron 52, 347–358 (2006).
- [48] Metzen, M. G., Hofmann, V. & Chacron, M. J. Neural synchrony gives rise to amplitude-and duration-invariant encoding consistent with perception of natural communication stimuli. *Front Neurosci* 14, 79 (2020).
- [49] Hofmann, V. & Chacron, M. J. Population coding and correlated variability in electrosensory pathways. Front Integr Neurosci 12, 56 (2018).
- [50] Grewe, J., Kruscha, A., Lindner, B. & Benda, J. Synchronous spikes are necessary but not sufficient for a synchrony code in populations of spiking neurons. *Proc Natl Acad Sci U.S.A.* **114**, E1977–E1985 (2017).
- [51] Fetcho, J. R., Higashijima, S.-i. & McLean, D. L. Zebrafish and motor control over the last decade. *Brain Res Rev* 57, 86–93 (2008).
- [52] Tabor, K. M. et al. Direct activation of the Mauthner cell by electric field pulses drives ultrarapid escape responses. J Neurophysiol 112, 834–844 (2014).
- [53] Orchard, G. et al. Hfirst: A temporal approach to object recognition. IEEE Trans Pattern Anal Mach Intell 37, 2028–2040 (2015).
- [54] Krebs, J. R., Kacelnik, A. & Taylor, P. Test of optimal sampling by foraging great tits. *Nature* **275**, 27–31 (1978).
- [55] Cerri, R. D. & Fraser, D. F. Predation and risk in foraging minnows: balancing conflicting demands. *Am Nat* 121, 552–561 (1983).
- [56] Kaelbling, L. P., Littman, M. L. & Moore, A. W. Reinforcement learning: A survey. *J Artif Intell Res* 4, 237–285 (1996).
- [57] Hitschfeld, É. M., Stamper, S. A., Vonderschen, K., Fortune, E. S. & Chacron, M. J. Effects of restraint and immobilization on electrosensory behaviors of weakly electric fish. *ILAR journal* 50, 361–372 (2009).
- [58] Roth, E., Zhuang, K., Stamper, S. A., Fortune, E. S. & Cowan, N. J. Stimulus predictability mediates a switch in locomotor smooth pursuit performance for *Eigenmannia virescens*. J Exp Biol 214, 1170–1180 (2011).
- [59] Vágvölgyi, B. P. General tracker. https://github.com/vagvolgyi/general_tracker (2021).
- [60] Biswas, D. et al. Data and code associated with the publication: Mode switching in organisms for solving explore-vs-exploit problem. Johns Hopkins Research Data Repository https://doi.org/10.7281/T1/QS3QFT6 (2023).